ARTICLE IN PRESS

Applied Energy xxx (xxxx) xxx–xxx

Contents lists available at ScienceDirect

Applied Energy

journal homepage: www.elsevier.com/locate/apenergy

Experimental investigation into the effectiveness of a super-capacitor based hybrid energy storage system for urban commercial vehicles

Ottorino Veneri[a,*], Clemente Capasso[a], Stanislao Patalano[b]

[a] Istituto Motori - CNR National Research Council, Via G. Marconi 4, 80125 Naples, Italy
[b] University of Naples, Federico II – DII, Fraunhofer JL IDEAS, P.le Tecchio 80, 80125 Naples, Italy

HIGHLIGHTS

- 1:1 scale laboratory test bench for electric power-trains supplied by hybrid energy storage systems.
- ZEBRA and super-capacitors based hybrid energy storage systems.
- Rule based energy management strategies.
- Laboratory experimental data on standard driving cycles.

GRAPHICAL ABSTRACT

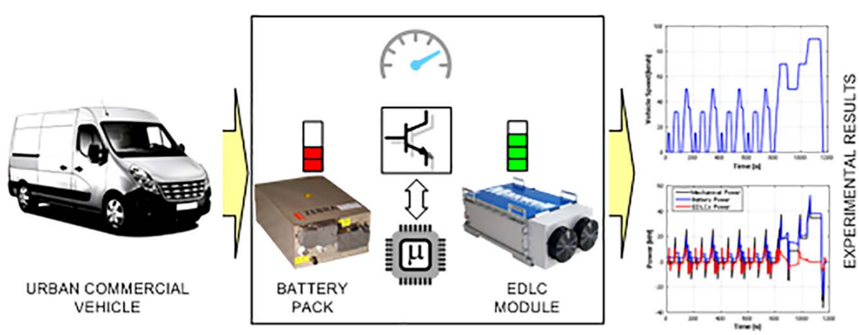

ARTICLE INFO

Keywords:
ZEBRA batteries
Electric vehicles
Electric double layer capacitors
Dynamic test bench
Hybrid storage systems
Energy management strategies

ABSTRACT

This paper is aimed to experimentally analyse the effectiveness of a hybrid storage system, when powering a commercial vehicle for urban use. The hybrid energy storage system is composed by two ZEBRA batteries, combined with an electric double layer capacitor (EDLC) module. The integration of those storage systems is obtained by means of a bidirectional DC/DC converter, which balances the electric power fluxes between batteries and super-capacitors, depending on the driving operative conditions. Modeling and simulations are preliminarily conducted with reference to the specific case study of an electric version of the Renault Master, supplied by the above described hybrid storage system. That theoretical activity allows the optimization of rule based energy management strategies for the hybrid energy storage system, in terms of the effectiveness in reducing the negative effects of high charging/discharging currents on battery durability. Then, the experimentation of the real power train, connected to the mentioned hybrid storage system, is carried out through a 1:1 laboratory test bench, able to perform the analysed energy management strategies on standard driving cycles, representative of the urban mission of the commercial vehicle under study. The obtained experimental results, expressed through electrical and mechanical parameters in a wide range of road operative conditions, show that the super-capacitors can improve the expected battery lifespan, with values of maximum effectiveness up to 52%, for driving patterns without negative road slopes. The procedure followed and presented in this paper definitely demonstrates the good performance of the evaluated hybrid storage system, controlled by the DC/DC power converter, to reduce the negative consequences of the power peaks associated with the urban use of commercial vehicles.

* Corresponding author.
E-mail address: o.veneri@im.cnr.it (O. Veneri).

https://doi.org/10.1016/j.apenergy.2017.08.086
Received 31 January 2017; Received in revised form 15 May 2017; Accepted 11 August 2017

Please cite this article as: Veneri, O., Applied Energy (2017), http://dx.doi.org/10.1016/j.apenergy.2017.08.086

Nomenclature

I'_{SC}	super-capacitors current on the DC-Link side of the DC/DC power converter output current
I'^{*}_{SC}	reference value of super-capacitors current on the DC-Link side of the DC/DC power converter
V_{DC}	DC-Link Voltage
V^{*}_{DC}	DC-Link Voltage Reference
I_{SC}	super-capacitor current
I^{*}_{SC}	super-capacitor current reference
I_{Batt}	battery current
I_{DC}	DC-Link current
V_{SC}	super-capacitor voltage
V^{*}_{SC}	super-capacitor voltage reference
I_{Th}	battery current saturation threshold
v	vehicle speed

1. Introduction

In recent years, automotive industry has largely focused the research and development investments on cleaner and more efficient road mobility solutions. These new interests were mainly encouraged by an increased awareness about environmental issues and natural oil depletion [1]. In this regard, plug-in hybrid and electric vehicles (PEVs) would represent an effective near-term option. In fact, this kind of vehicles is expected to reduce fossil fuel dependency with positive effects on air quality, public health and global warming [2–3].

In addition, the development of PEVs, in their different uses for both private and corporate activities, has been further supported by recent improvements in the Energy Storage System (ESS) technology. In fact, new lithium based electrochemical batteries present good performance in terms of energy density and safety. This allows new generation of PEVs, powered by lithium battery pack, to satisfy the great part of vehicle owners' needs, especially in terms of ensuring a suitable driving range [4]. On the other hand, the mission of urban road vehicles is generally characterized by variable power demand, with peak values to be supplied or recovered by on-board ESS, during frequent acceleration and deceleration phases [5]. These are the reasons why ESS are required to be characterized by both high specific power and high energy density. Unfortunately, current battery technologies are not able to simultaneously satisfy both of these requirements. In fact, recent technologies of high specific power storage devices are still characterized by low performance in terms of energy density. In addition, high charging-discharging rates generally result in negative effect on battery efficiency, internal resistance and durability in terms of life-cycle [6–7].

The use of on-board Hybrid Energy Storage Systems (HESS), which combine the performance of electrochemical batteries with high specific power storage devices, is becoming a key point of interest for the scientific literature [8–10]. In particular, super-capacitors, also known as Electrochemical Double Layer Capacitors (EDLCs), present relevant advantages, which encourage more and more their use in automotive applications. Those advantages mainly consist in the possibility for the EDLCs to store a higher amount of electric energy, in comparison with traditional capacitor technologies, and to supply/receive higher values of electric power, in comparison with electrochemical battery technologies [11–13]. Moreover, EDLCs are characterized by long cycle life, supporting hundreds of thousands of complete charging/discharging cycles, with minimal change in their performance [14]. This is due to the fact that, although EDLCs are considered electrochemical devices, no chemical reaction is involved in their charging and discharging operations. EDLCs chemical composition is based on the presence of a conductive electrolyte salt in direct contact with the metal electrodes, whereas a separator provides insulation and allows ions transfer between the electrodes. Each electrode is realized with a porous activated carbon material, obtaining very high values of energy density with equivalent active areas up to 2000 m^2/cm^3. The rated cell voltage is 2.6 V [15].

Various solutions can be analysed for the integration of battery and EDLCs in the on-board hybrid energy storage systems. In this regard, the main power architectures, supporting the above integration are described in [16] and in [17], with specific focus on their related advantages and drawbacks in terms of cost, flexibility and efficiency. In particular, the direct parallel connection between EDLCs and battery pack represents a cheap solution to reduce fast transient in battery charging/discharging current. On the other hand, this solution makes impossible for the HESS to take advantage of the complete EDLCs voltage range. In addition, the external control of power fluxes between the two storage systems cannot be supported by this configuration. For this reason, a bidirectional DC/DC converter, interfacing EDLCs with battery pack is generally proposed in the literature as a more flexible solution. This solution, also known as UC/battery configuration, enables the evaluation of various energy management strategies, which can be performed through the proper control of the above converter. In addition, the converter can work in step up or step down mode, in order to use the whole EDLCs voltage range during their charging/discharging operations. This configuration involves higher costs, due to the high power bidirectional DC/DC converter, which is required to support the charging/discharging power of EDLCs. Cao and Emadi [17] also propose the use of new power architecture, where the integration between battery and super-capacitors is realized through the use of a bidirectional DC/DC converter which works in parallel connection with a controlled switching device.

Further studies, available in the scientific literature, are focused on energy management strategies of HESS. In particular, heuristic energy management strategies are proposed in [18–20], highlighting the effectiveness of super-capacitors in increasing the durability of the vehicle battery pack, when they are used in urban driving cycles. Ziyou et al. [21] analyse a multi-objective optimization algorithm, which is aimed to simultaneously minimize the cost of a hybrid energy-storage unit and the capacity loss of a $LiFePO_4$ battery pack, for a specific road electric vehicle running on typical urban driving cycles. A novel dynamic programming analysis method is proposed by Zhang et al. [22], in order to maximize efficiency and durability of the whole storage system. The proposed method is verified for different values of battery State of Charge (SoC) and State of Health (SoH). A novel energy management strategy in hybrid storage systems is also described in [23] by Carter et al. In this case, the authors develop a tunable strategy, which is able to achieve two separate goals. The first goal is the improvement of vehicle efficiency and autonomy, whereas the second goal is the reduction of current peak values for the battery pack, with positive consequence on the expected battery life.

The referred state of art is focused on the analysis of energy management strategies, whose goals are mainly related to increasing battery durability, vehicle autonomy and overall vehicle energy conversion efficiency. The effects of the proposed strategies are generally evaluated through modeling and simulation activities.

On the base of the above scientific literature analysis, this paper is aim to cover the lack of experimental knowledge about the positive effects of EDLC based hybrid storage systems, working in real operative conditions. For this reason, the main contribution of this paper is focused on the experimental assessment of specific energy management strategies, which maximize the effectiveness of a hybrid energy storage system, when supplying a real electric propulsion system for urban vehicles. Those strategies are preliminary evaluated and optimized through the use of simulation environment. Then the proposed activity is carried out through a 1:1 scale laboratory test-bench, able to simulate vehicle inertia and road resistant forces on standard driving cycle.

The remainder of the paper is organized as follows. Starting from a description of the main characteristics and components of an urban commercial vehicle, considered as case study, different energy management strategies of the on-board HESS, which optimize the battery pack lifespan, are proposed in Section 2. In Section 3, a quasi-static model of the vehicle is used to tune the working parameters of the above strategies and to obtain preliminary results, before running experimental tests. Then, in Section 4 the laboratory test bench is described, with particular focus on the DC/DC bidirectional power conversion system, which realizes the integration between EDLCs and ZEBRA batteries. Finally, in Section 5 a wide range of experimental results and related effectiveness values are described and commented. These results concern the vehicle propulsion system, supplied by the HESS and running on the test bench, under various operative conditions. The conclusions of the paper are presented in Section 6.

2. Case study and energy management strategies

2.1. Case study

The considerations formulated in this section can be applied for all kinds of urban electric vehicles. For the sake of simplicity, a specific case study of full electric urban vehicle is analysed in this paper. This case study is based on a full electric version of the Renault Master, which has been already considered in a previous paper by the authors of this work, in order to evaluate the performance of that vehicle, when supplied only by a Zebra battery pack [24]. For this reason, the main parameters and characteristics of the vehicle are reported in the above paper. The electric drive of the vehicle is supplied, in this case, by a HESS, which is composed of electric double layer capacitors (EDLCs) and ZEBRA batteries. The onboard integration between the above storage systems is performed through a bidirectional DC/DC power converter, on the base of the well-known UC/battery configuration, proposed and described in [17]. The use of this configuration simplifies the integration of EDLCs with the existing storage system, which is based on a ZEBRA battery pack, without involving any change in the DC-Link operative voltage range supported by the electric drive. In addition, this configuration simplifies the control of power fluxes between the two storage units, which can be realized through the DC/DC bidirectional converter. The block scheme of the considered vehicle, supplied by the HESS is depicted in Fig. 1.

The battery pack is composed of two 550 V to 38 Ah ZEBRA batteries, which are electrically connected in parallel on the DC-Link side of the electric drive. Each ZEBRA battery is realized with strings of 216 cells. The main characteristics of the considered ZEBRA battery pack are reported in Table 1.

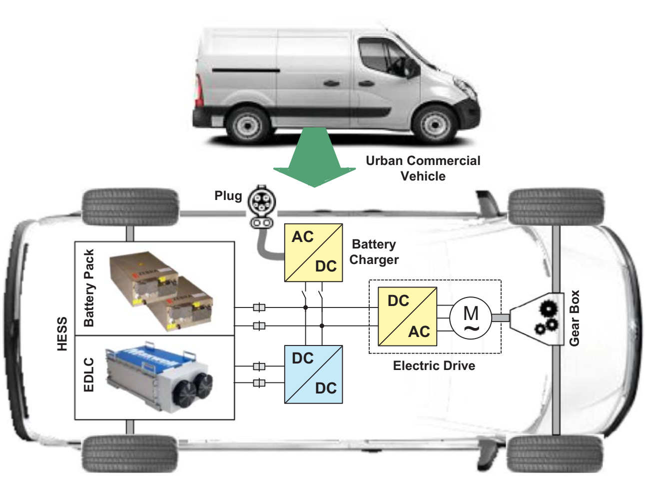

Fig. 1. Block scheme of the vehicle propulsion system supplied by the HESS.

Table 1
Main characteristics of the ZEBRA battery pack.

Rated Capacitance (Ah)	76
Open circuit voltage (V)	557
Peak discharging current (A)	224
Working temperature range (K)	508–613
Number of cells	2x216
Maximum Stored Energy, Individual Cell (W h)	98

Table 2
Main characteristics of the EDLC module.

Rated Capacitance (F)	63
Min. initial Capacitance (F)	63
Max. initial Capacitance (F)	76
DC Equivalent Series Resistance (mΩ)	18
Rated Voltage (V)	125
Absolute Max. Voltage (V)	136
Absolute Max. Current (A)	1900
Capacitance of Individual Cells (F)	3000
Maximum Stored Energy, Individual Cell (Wh)	3.0
Number of Cells	48

For this specific case study, the storage system, based on the ZEBRA battery pack, is integrated with a 63 F to 125 V EDLCs module. The main characteristics of this module are reported in Table 2.

In particular, the EDLCs module is realized with 48 cells of 3000 F, which are electrically connected in series. Whereas, the low value of DC equivalent series resistance of 18 mΩ involves high performance of the module in terms of maximum charging/discharging current.

The control system of the DC/DC power converter is designed to support simulation and laboratory activities related to identification, analysis and test of energy management strategies, for the HESS of the considered vehicle. The main scheme of reference and actual parameters involved in the DC/DC power converter control, are reported in Fig. 2.

Three different control modes are considered for the embedded board of the power converter [25]. The logic scheme of these control modes is shown in Fig. 3.

The first power converter control mode, which is referred as I_{SC} *control mode*, is based on the reference value, I^{*}_{SC}, of the EDLCs current. In this case, a feedback loop control scheme allows the EDLCs current, I_{SC}, to follow the above reference value through the PWM modulation of the power converter. This control mode is useful to perform charging/discharging tests of EDLCs with predefined I_{SC} current profile.

The I'_{SC} *Control Mode* works on the base of the reference value of the converter current, I'^{*}_{SC}, evaluated on the DC-Link side. As clear from

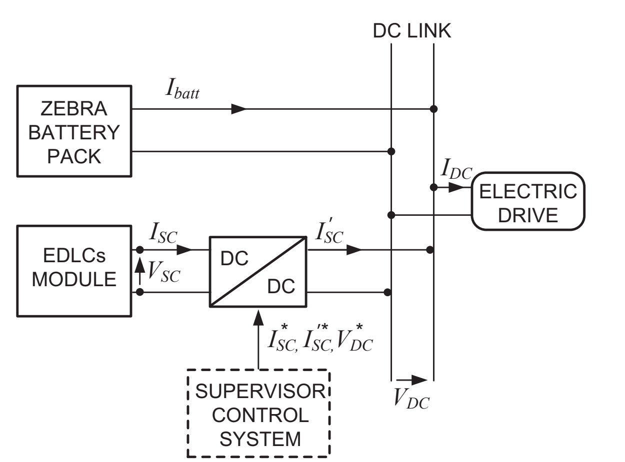

Fig. 2. Main Scheme of the hybrid storage system with reference and actual electric parameters.

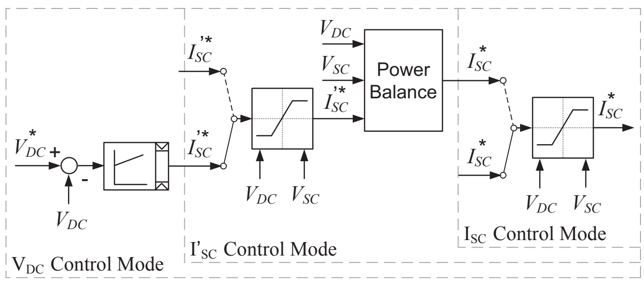

Fig. 3. Logic scheme of the three control modes supported by the DC/DC power converter.

Fig. 3, this control is performed by including the I_{SC} control mode after the power balance block. In fact, the equivalent value of I^{*}_{SC} can be calculated by using the Eq. (1), which is obtained from the input/output power balance of the converter, supposing that no power losses are caused by the DC/DC converter operations.

$$I^{*}_{SC} = \frac{V_{DC} I'^{*}_{SC}}{V_{SC}} \tag{1}$$

This control mode can be used for a direct power fluxes management, on the DC-Link side, between battery pack and EDLCs module.

The last control mode, referred as *V_{DC} Control Mode*, is based on the DC-Link reference voltage value, V^{*}_{DC}. As reported in Fig. 3, this mode is realized through a PI controller, which compares the actual value of DC link voltage, V_{DC}, with its reference value, V^{*}_{DC}. The output of the PI controller, evaluated on the base of that comparison, is then used for the *I'_{SC} Control Mode*. In this way, the DC link voltage, V_{DC}, can be controlled through charging/discharging operations of EDLCs, with a maximum EDLCs current, I_{SC}, which is set at a predefined saturation value.

The DC/DC converter control system also performs over-voltage and under-voltage protections for the EDLCs module. In this regard, the dynamic saturation blocks, reported in Fig. 3 are representative of minimum and maximum voltage thresholds and limits, which can be defined on the base of EDLCs characteristics. In case the EDLCs voltage reaches one of those threshold values, the EDLCs charging/discharging current is linearly reduced, to obtain a null value, when the related voltage limit is reached.

2.2. Energy management strategies

As mentioned in the Introduction Section, Energy Management Strategies (EMSs) for hybrid storage systems can pursue different objectives, which are generally related to vehicle performance and cost optimization. In this regard, taking into account the urban mission of the selected vehicle, the EMSs considered in this paper, are focused on the optimization of battery durability. As well known, the battery durability is affected by a large number of parameters, which generally depends on environmental and operative conditions. ZEBRA batteries are characterized by very high values of working temperature, which is required by the fuse electrodes. For this reason, those batteries are provided with thermal insulation and, therefore, environmental effects on the battery pack durability can be consequently neglected. On the other hand, urban driving paths present frequent acceleration and deceleration phases, involving high values of battery charging/discharging current, which have recognized effects on the battery durability. These effects, as suggested in different papers [18,20,26,27], can be limited by reducing the mean square value of charging/discharging battery current, evaluated for a specific working cycle. As a consequence, a durability loss function related to the battery charging/discharging current values can be calculated through the Eq. (2).

$$L(T) = \frac{1}{T}\int_0^T |I_{Batt}|^2 dt \tag{2}$$

where T is the time duration of the considered working cycle. The effectiveness evaluation for each EMS can be performed by considering the relative difference between the loss function of onboard storage system without EDLCs, $L_{Batt}(T)$, and the loss function of the on-board hybrid energy storage system, $L_{HESS}(T)$. Therefore, the effectiveness of the generic energy management strategy, EMS_n, is given by the following Eq. (3).

$$Eff_{EMS,n}(T) = \frac{L_{Batt,n}(T) - L_{HESS,n}(T)}{L_{Batt,n}(T)} \cdot 100 \tag{3}$$

It is clear that, for a specific driving cycle, the higher is the effectiveness value the higher is the contribution of EDLCs in reducing the effects of high charging/discharging current values on the battery durability. For this reason the main objective of the EMSs analysed in this paper are aimed to maximize the effectiveness value reported in the Eq. (3).

The first EMS, considered in this section, has been proposed in [18] and it is based on the saturation of the battery current value, I_{Batt}. In this case, the current required by the electric drive, I_{DC}, is supplied by the on-board battery pack until it reaches a threshold value, I_{Th}, which has been preliminarily defined. Then, the difference between the current required by the electric drive, I_{DC}, and the saturated battery current, I_{Th}, is supplied by the super-capacitors through the DC/DC power converter, which is controlled in *I_{SC} control mode.* With this EMS, the regenerative operations are controlled by setting the DC/DC current reference, I'^{*}_{SC}, equal to the current value required on the DC-Link side by the electric drive, I_{DC}. As a consequence, the regenerative current is almost completely used for the charging operations of the EDLCs module, reducing in this way the effects of regenerative operations on battery durability. In the following this strategy is referred as *Th Strategy*.

The functional principle of the *Th Strategy* can be synthesized as depicted in Fig. 4.

The value of the parameter I_{Th}, can be optimized in the simulation environment, through a recursive evaluation of Eq. (3) for different values of I_{Th}, with the vehicle running on a specific driving cycle.

The second EMS is based on the evaluation of *Exponential Weighted Moving Average* (EWMA) for the current required by the electric drive, I_{DC} [19]. This value, for the *k-th* element, is indicated with $\bar{I}_{DC,k}$ and can be defined through the Eq. (4).

$$\bar{I}_{DC,k} = \alpha \cdot I_{DC,k-1} + (1-\alpha) \cdot \bar{I}_{DC,k-1} \tag{4}$$

where α epresents the *decay factor* and its value is in the range [0, 1]. A reduction of durability losses for the battery pack, could be reached by assuming that the value of $\bar{I}_{DC,k}$ is supplied by the battery pack, whereas

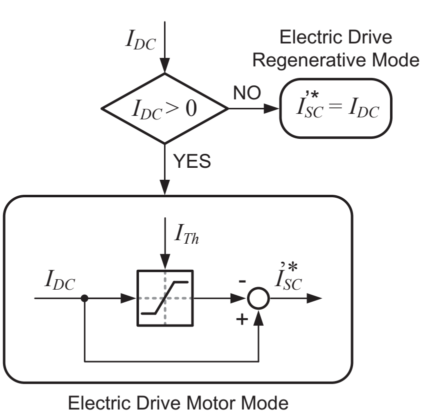

Fig. 4. Functional principle of the Th Strategy with the electric drive in regenerative mode (NO) and in motor mode (YES).

the remaining part of the required current, $I_{DC,k} - \bar{I}_{DC,k}$, can be supplied by the EDLCs. As a consequence, the DC/DC power converter current reference, for the *k-th* element, $I'^{*}_{SC,k}$, is given by the following Eq. (5).

$$I'^{*}_{SC,k} = I_{DC,k} - \bar{I}_{DC,k} \tag{5}$$

Also for this EMS, the choice of the parameter α, on a specific driving cycle, can be optimized in simulation environment, through the recursive evaluation of Eq. (3). In the following, this strategy is referred as *EWMA Strategy*.

The last EMS [20] is based on the assumption that peak values of charging/discharging current, for the onboard storage systems, are generally related to the contribution of vehicle inertia during transient acceleration and deceleration phases, related to the urban mission of the considered vehicle. In addition, the charging/discharging operations of EDLCs can be optimized by considering their voltage as a function of the vehicle speed. In the following, this strategy is referred as Ke Strategy. For this EMS, the evaluation of the DC/DC power converter current reference, I'^{*}_{SC}, can be carried out on the base of the calculated battery current reference, I^{*}_{batt}. This last value is composed by two terms. The first term, $I^{*'}_{batt}$, depends on the resistant forces, which are related to road and vehicle characteristics. In fact, the variability of this kind of forces is generally low and, for this reason, they can be supplied by using the energy coming from the battery pack, without involving substantial effects on its durability. As a consequence, this first term can be expressed as a function of the mechanical resistant power, P^{res}_{mech}, and of the DC-Link voltage, V_{DC}, on the base of the Eq. (6).

$$I^{*'}_{batt} = f(P^{res}_{mech}, V_{DC}) = \frac{P^{res}_{el}}{V_{DC}} \cdot \eta_{el} \tag{6}$$

where η_{el} is the electric drive efficiency, P^{res}_{el} represents the electric power related to road and aerodynamic resistant forces. For the evaluation reported in this paper, the value of η_{el} is derived by the electric drive efficiency map reported in [24].

The second term of battery current reference, $I^{*''}_{batt}$ is calculated taking into account that the EDLCs module should be ready to accept the available vehicle kinetic energy, during regenerative operations, and to supply peak power, during the acceleration phases required by the considered driving cycle. For this reason, an EDLCs voltage reference value, V^{*}_{SC}, can be evaluated by considering the sum of vehicle kinetic energy and electric energy stored in EDLCs equals to a constant value k, as reported in the Eq. (7) [20]

$$\frac{1}{2}C(V^{*2}_{SC} - V^{2}_{\min}) + \frac{1}{2}mv^{2} = k \tag{7}$$

where V_{min} represents the minimum voltage value of the EDLCs module. The value of k can be derived by the consideration that the EDLCs should be fully charged when the vehicle speed is equal to 0. Therefore, the relationship between vehicle speed and EDLCs voltage reference, V^{*}_{SC}, can be evaluated with the following Eq. (8) as a function of vehicle speed.

$$V^{*}_{SC} = f'(v) = \sqrt{V^{2}_{\max} - \frac{m}{c}v^{2}} \tag{8}$$

where V_{max} represents the EDLCs maximum voltage. On the base of the above evaluations, the second term of the battery current reference, $I^{*''}_{batt}$, is obtained through a PI controller, which compares the EDLCs actual voltage, V_{SC}, with its reference value, V^{*}_{SC}. As a consequence, the reference signal for the DC/DC converter current, I'^{*}_{SC}, comes out from the block scheme reported in Fig. 5.

In this case, the parameter k_i and k_p of the PI controller can be optimized in simulation environment on the base of the Eq. (3).

3. Modeling and simulation results

A simplified vehicle model has been developed, in Matlab-Simulink environment, in order to perform preliminary evaluations on the effectiveness of the EMSs described in the precious section, for specific urban driving cycles. This model is based on simulation blocks, related to vehicle, road resistant forces and driver, which have been modeled with the quasi-static approach described in a previous paper published by the authors [24]. For the evaluations reported in this paper, the above numerical model has been extended, by taking into account the integration of EDLCs with the ZEBRA battery pack through the use of a bidirectional DC/DC power converter. In particular, the EDLCs model is based on the *classical equivalent circuit*, described in [15]. This circuit includes a capacitance *C*, an Equivalent Series Resistance (ESR), which is representative of a loss term that models the internal heating of the capacitor, and an Equivalent Parallel Resistance (EPR), representative of current leakage effect [28]. As reported in [15], the C-EPR time constant is generally quite large and the EPR can be consequently neglected in case of short charging/discharging times. The mission of the vehicle proposed in this paper is referred to an urban use, which is characterized by frequent short transient deceleration and acceleration phases. For this reason, only the capacitance *C* and the *ESR* are considered in the EDLCs equivalent circuit. The value of *C* and *ESR* can be obtained by the datasheet of the EDLCs, which are summarized in Table 2.

The DC/DC bidirectional power converter is modeled as an ideal device, which manages the power exchange between the battery pack and EDLCs on the base of the required operative conditions. In this case, an ideal controlled current source is used, in order to set the EDLCs current, I_{SC}, on the base of its reference value, I^{*}_{SC}, obtained through the selected control mode. The simulation scheme of EDLCs with the DC/DC converter and the related control modes are depicted in Fig. 6.

The DC/DC converter current on the DC-link side, I'_{SC}, is evaluated on the base of the ratio between DC link voltage, V_{DC}, and EDLCs voltage, V_{SC}, since no power losses are considered for the power converter operations. The limitation of the current reference, I^{*}_{SC}, is performed through a dynamic saturation block, which operates on the basis of the EDLCs voltage, V_{SC}.

For the simulation and experimental tests presented in this paper, the EDLCs module has been preliminary discharged at the intermediate voltage value of 95 V. In addition, the parameters reported in Table 3 have been set in the power converter control software.

The use of simulation environment simplifies the optimization of the EMSs, analysed in the previous section, for the vehicle running on urban driving cycles. In fact, the proposed model allows the investigation of a wide range of values, associated with the parameters I_{Th}, α, k_p, k_i of the considered EMSs, and the evaluation of the related *effectiveness*, on the base of the Eq. (3). In this way, the optimal parameters, which maximize the effectiveness of each EMS can be found through an iterative simulation procedure. This procedure has been carried out for the vehicle under study, running on both ECE-15 and NEDC driving cycles, since these two kinds of cycles are generally chosen as representative of urban driving paths. Various road slopes have been also analysed for the ECE-15 driving cycle, whereas the only case of plain road has been considered for the NEDC driving cycle. This

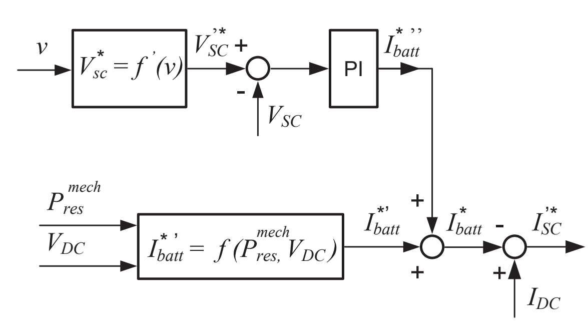

Fig. 5. Block scheme of the Ke strategy.

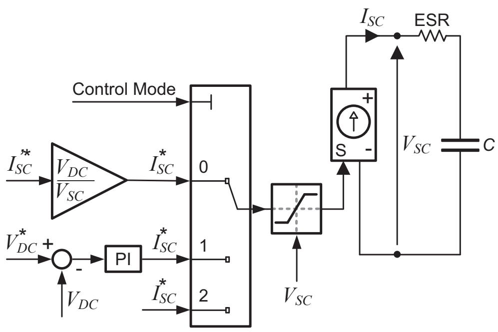

Fig. 6. Simulation scheme of EDLCs with the DC/DC converter.

Table 3
Parameters of the DC/DC power converter software for the experimental tests.

Maximum EDLCs Voltage Limit [V]	130
Maximum EDLCs Voltage Threshold [V]	125
Minimum EDLCs Voltage Threshold [V]	40
Minimum EDLCs Voltage Limit [V]	35
Maximum EDLCs Charging Current Limit [A]	100
Maximum EDLCs Discharging Current Limit [A]	−100
Control Mode	I'_{SC} Control Mode

choice is justified by the fact that, the extra-urban part of the NEDC cycle, at 90 km/h with positive or negative road slope, is not considered as significant for the urban mission of the vehicle under study. Each step of the optimization procedure has been carried out on the base of five consecutive repetitions of the driving cycle under study, which are required for a stable evaluation of the EMS effectiveness. In Table 4 the optimal parameters obtained through the above procedure are reported.

With reference to the above parameters, the maximum effectiveness values of 57% and 16% have been respectively obtained for the NEDC and ECE 15 driving cycles, on plain road, selecting the *Ke Strategy.* In addition, the best effectiveness of 37% has been obtained for the ECE 15 driving cycle, on a road slope of 5%, with the *EWMA Strategy*.

An example of the results that is possible to obtain, by using the numerical model with the optimized parameters for the NEDC driving cycle ($k_p = 0.25$; $k_i = 0.0025$), is reported in the following Fig. 7, for the specific case of the *Ke Strategy*,

From the results reported in the above Figure, it is possible to observe that, during the first 800 s, which represent the urban part of the NEDC driving cycle, the use of EDLCs reduces of about 20% the electric power peaks supplied by the battery pack, with respect to the total mechanical power that is supplied by the electric drive towards the power train. On the other hand, during the last part of the cycle, the limitation, imposed by the DC/DC converter on the maximum EDLC charging/discharging current values at about 100 A, reduces the electric power coming out of the EDLC for both transient and steady state phases. This behaviour of the hybrid storage system, in the last phase of the driving cycle, justifies the low value of effectiveness of 16% for the NEDC driving cycle, in comparison with the effectiveness of 57% reported for the case of ECE-15 cycle, only composed by the urban part of NEDC.

The above evaluations show the convenience of using a quasi-static numerical model, representative of the behaviour of the considered vehicle, supplied by a hybrid energy storage system, to analyse optimized energy management strategies. In fact, as demonstrated in this paper, preliminary and useful results can easily be obtained for various driving cycles, before running experimental tests on the real powertrain at the test bench. This procedure results very efficient because it permits the convenient reduction of experimentation time, risks of damages and general costs to obtain engineering results.

Table 4
EMSs parameters evaluated through the optimization procedure.

EMS	Parameters	ECE-15	ECE15 5%	NEDC
Th Strategy	I_{Th} [A]	10	50	12
EWMA Strategy	α	0.033	0.017	0.064
Ke Strategy	k_p	1	1	0.25
	k_i	0.0025	0.025	0.0025

4. Experimental set-up

A 1:1 scale laboratory test bench has been set-up in order to experimentally evaluate the effectiveness of the proposed hybrid storage system, when supplying an electric propulsion system in real operative conditions. The block scheme of the laboratory test bench is shown in Fig. 8.

A detailed description of the main components realizing the test bench is reported in a previous paper published by the authors [24].

In this case, the laboratory test bench has been extended to perform the integration of the existing ZEBRA battery pack and EDLCs in a hybrid energy storage system. The integration is realized by means of a DC/DC bidirectional power converter, which interfaces the EDLCs module with the DC-link. The main characteristics of the power converter are reported in Table 5.

From the above table, it is clear that the maximum current value, admitted by the power converter on the SC side, is lower than the maximum allowed current for the EDLCs module, reported in Table 2. This current limitation involves a reduction in the available charging/discharging electric power of the EDLCs module. However, taking into account the power requirements, related to the urban mission of the considered vehicle, that reduction is acceptable for the analysed EMSs of this paper. The above converter is based on a three-phase interleaved full bridge power architecture, where the three legs, on the SC side, are electrically connected in parallel by means of three identical 2.23 mH/100 A inductances, L_u, L_v, L_w. The electrical scheme of the bidirectional DC/DC power converter is reported in Fig. 9.

The main advantages of the above described power architecture, consist in a relevant reduction of DC-Link current ripple and of rms current values for the power electronic devices, in comparison with similar solutions based on single phase schemes [29,30]. The embedded control board allows the power converter operating in the control modes I_{SC}, I'_{SC}, V_{DC}, considered in the case study sub-section, through the PWM modulation of the six IGBTs. The control mode can be chosen by the user through a computer software interface, which interacts with the converter control board via ModBUS communication. The reference values I^*_{SC}, I'^*_{SC}, V^*_{DC} can be set by the operator, or by an external control system of higher hierarchical level, through analogue voltage signals. The good performance of the power converter in following the electric reference values, in the above considered control modes, have been verified and evaluated in a paper previously published by the authors [25].

The EDLCs module, produced by Maxwell Technology®, is equipped with an embedded monitoring system, which uses an 8-pin Deutsch connector for CAN bus Communication. In particular, that system, starting from the negative terminal of the EDLCs module, performs voltage measurements on 6 consecutive strings, composed by 8 cells connected in series, and transmits the obtained values towards the CAN network. A warning flag is also sent towards the CAN network if the voltage difference among the 8-cell strings is greater than 3 V. In this way, it is possible to avoid voltage unbalance conditions, which could reduce the durability of the EDLCs module.

The monitoring system also provides thermal protection for the module. In fact, its operative temperature is controlled by the monitoring system, by means of two 24 V DC axial cooling fans, which are activated on the base of the measurements obtained with a PT 100 RTD temperature sensor.

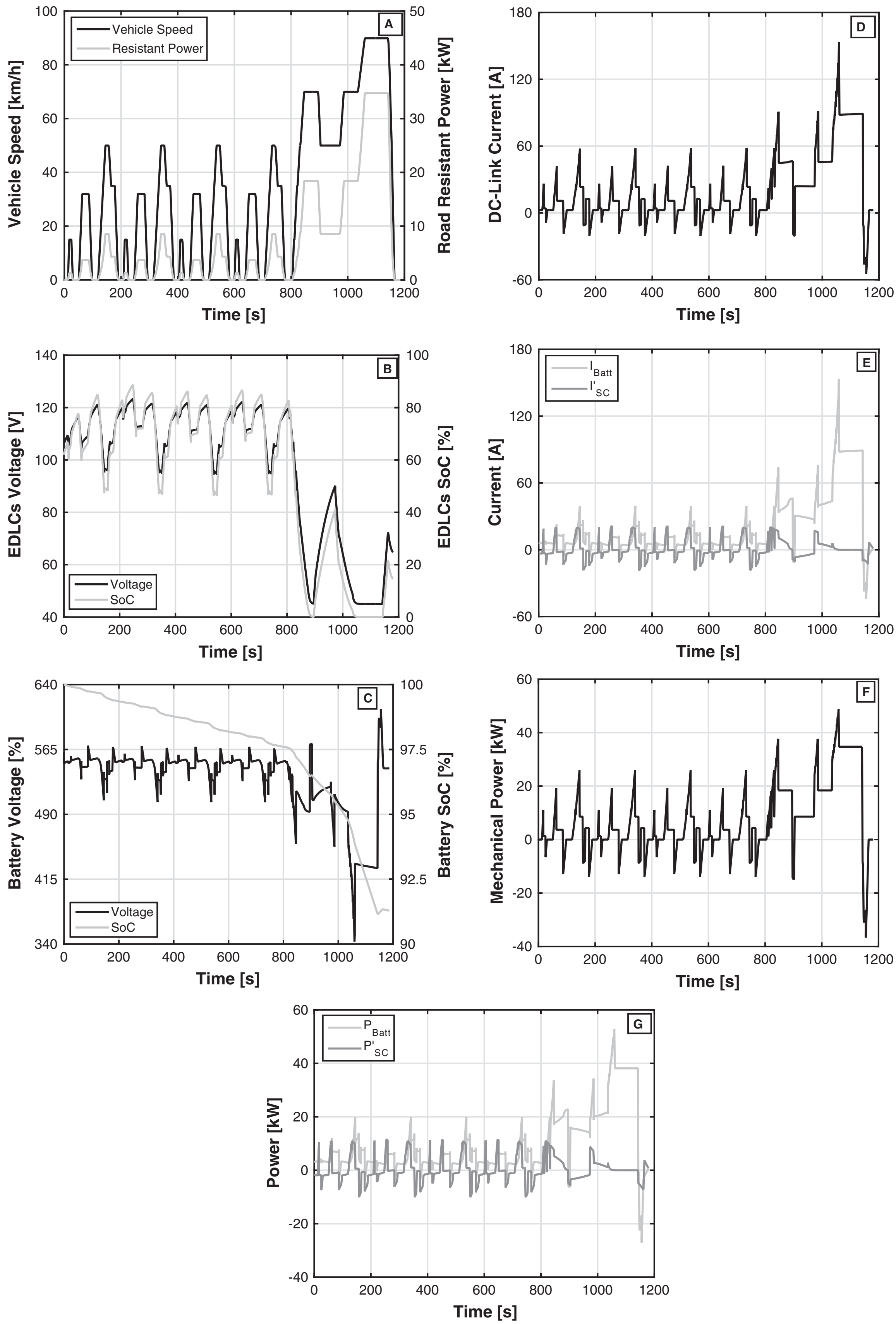

Fig. 7. Simulation results: Vehicle Speed and Road Resistant Power (A), EDLCs Voltage and SoC (B), Battery Pack Voltage and SoC (C), DC-Link Current (D), Battery and EDLCs current on the DC-Link side (E), Mechanical Power (F), Battery and EDLCs power on the DC-Link side (G) vs. time for the NEDC driving cycle with Ke Strategy.

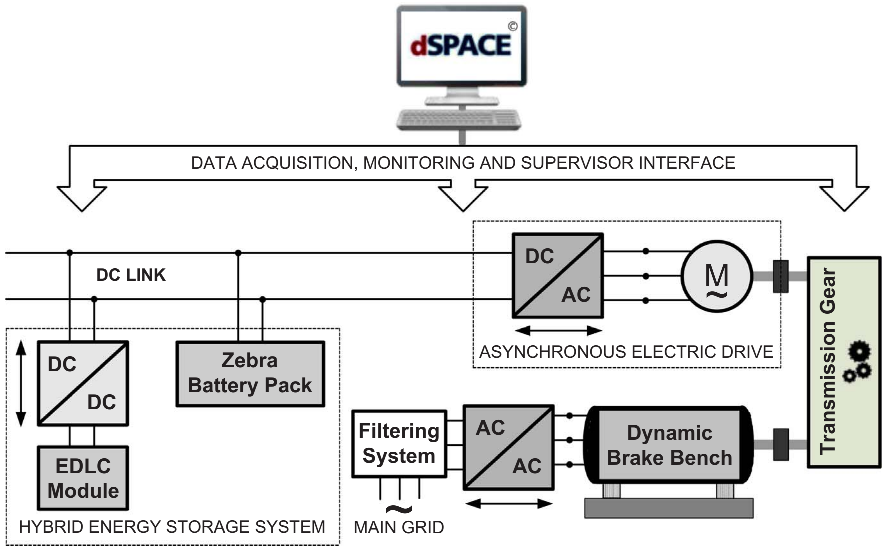

Fig. 8. Block scheme of the laboratory test bench.

Table 5
Main characteristics of the DC/DC power converter.

Min Voltage/DC Link-side [V]	333
Max Voltage/ DC Link-side [V]	828
Rated current/ DC Link -side [A]	150
Rated current/SC-side [A]	100
Max current/SC-side [A]	100
Switching frequency [kHz]	2.5–5

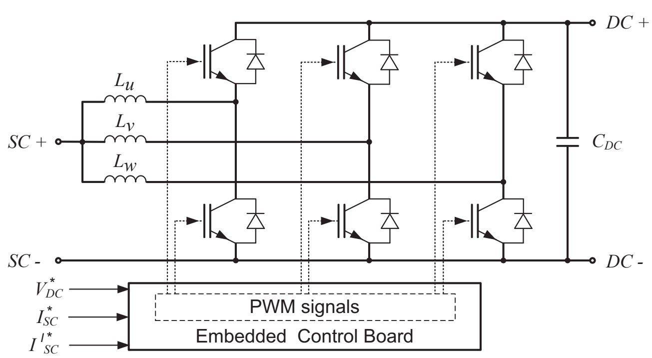

Fig. 9. Electric scheme of the DC/DC bidirectional converter.

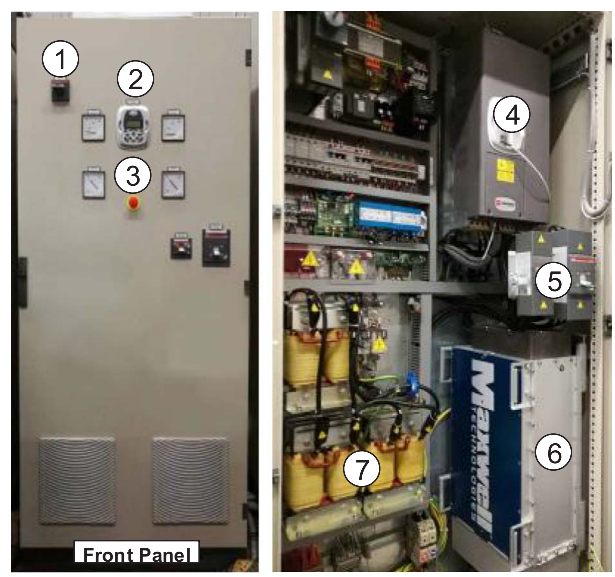

Fig. 10. Picture of the EDLCs module laboratory rack: (1) main switch; (2) LCD display of the DC/DC converter; (3) front panel measures; (4) DC/DC converter; (5) circuit breakers; (6) EDLCs module; (7) DC/DC converter inductances.

The DC/DC power converter and EDLCs module have been integrated in a laboratory rack, which includes converter inductances, measurement and protection components. A picture of this rack is shown in Fig. 10.

In particular, the main switch (1) allows the connection of the power converter auxiliary systems related to sensors and LCD display, with single-phase 230 V AC voltage. The LCD display (2) is used for the monitoring and visualization of the DC/DC converter operative conditions, in terms of selected control mode and reference voltage/current values. A front panel analogic measurement system (3) allows the user receiving fast information related to EDLCs and DC-Link voltage/current. In addition, the laboratory rack, with its components, can be easily included/excluded from the test bench by using circuit breakers (5), which are located on the DC-Link side and on the SC side of the DC/DC power converter.

As reported in the test bench scheme of Fig. 9, the vehicle propulsion system, supplied by the hybrid energy storage unit, is coupled with a dynamic electric brake, through a 1:3.17 gear transmission ratio. The use of that brake allows the simulation of road resistant forces on standard driving cycles, on the base of the main road and vehicle parameters. In addition, the electric brake, with its control system, also performs the simulation of vehicle inertia, during the acceleration phases and regenerative operations, required by the driving cycles. This aspect is particularly relevant for experimental tests, related to the EMSs proposed in the Section 2. In fact, the highest values of charging/discharging current are evaluated, through the simulation environment, during acceleration and deceleration phases.

The control of the electric brake is based on a bidirectional power conversion system, which is connected to the low voltage three-phase AC-Grid. In this case, two separate AC/AC power converters, are both involved in the control of the brake asynchronous machine. In fact, the brake can be controlled both as a motor, when the electric energy is supplied by the main grid, and as a generator, when the electric energy is fed back toward the main grid.

A picture of the laboratory rack, including the brake control system, is shown in Fig. 11. In particular, the above control system (1) is integrated in the laboratory rack, together with filtering systems (2), which have been included in order to meet the power quality levels

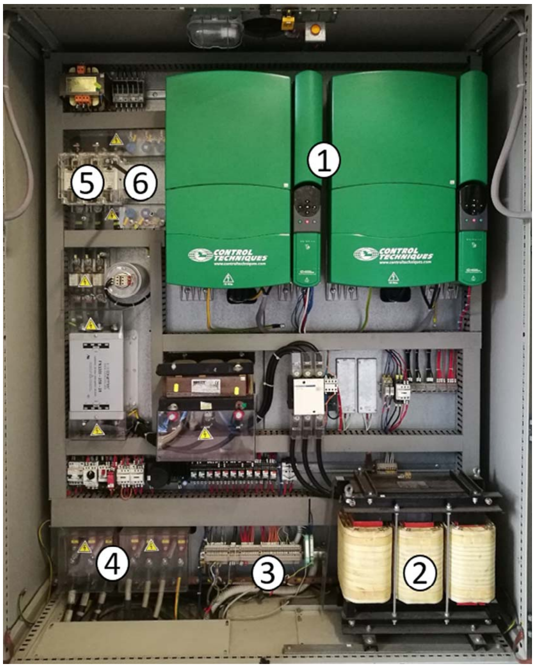

Fig. 11. Picture of the dynamic brake control rack: (1) bidirectional power conversion system; (2) filtering system; (3) measurement and control signals; (4) three-phase ac grid power cables; (5) fuses; (6) main switch.

required by the Grid System Operator, measurement/control signals (3) and protection systems (5, 6).

For the experimental tests reported in the next Section, the decelerating phases, required by the driving cycles, are carried out, without the simulation of the vehicle mechanical brakes. This choice involves lower performance of the test bench in following the speed profile required by the driving cycle, during the decelerating phases. On the other hand, the consequent reduction of mechanical losses allows the optimization of energy recovery in the hybrid energy storage system. For this reason, the decelerations required by the driving cycles are performed through the control of vehicle electric drive, which can work either in motor or in generator mode. In fact, the electric drive bidirectional control system allows regenerative operations on the base of two possible torque-speed characteristics, which are referred as *braking* and *decelerating* profile. Those characteristics are reported in Fig. 12.

The decelerating torque profile can be modified via the remote control software of the electric drive. In fact, the maximum decelerating torque, $T_{dec,\max}$, is set as proportional to the maximum braking torque, $T_{br,\max}$, through a factor k, in the range [0–1]. On the base of the deceleration values, required by the driving cycle, the vehicle speed can be regulated by using either braking or decelerating torque profile. This choice is performed by the control system through a digital input of the electric drive.

As reported in Fig. 8, the laboratory test bench is managed by means of a programmable dSpace device. The use of that device makes easy the deployment of the EMSs in the control system of the experimental test bench. In fact, those EMSs have been preliminary evaluated in simulation environment, with the possibility for the Simulink blocks to be implemented in the real time processor of the dSpace device. This operation can be performed in a fast way through the use of Real Time Interface (RTI) libraries. Those libraries, starting from Simulink blocks, automatically generate the C code to be compiled on the real-time hardware of the dSpace device. For the experimental tests presented in the next section, analogue output voltage signals have been used to control the reference values of each control mode supported by DC/DC bidirectional converter. Electric and mechanical parameters of the test bench are acquired through analogue voltage input signals, coming from the related sensors, located on the test bench. Specific operative information related to battery pack and EDLCs module (i.e. voltage unbalance warning, operative temperature, state of charge, etc.) is acquired through a CAN communication bus, which interfaces the dSpace device with the MBS (Multiple Battery control System) of the ZEBRA battery pack and the monitoring system of the EDLCs module.

The acquired data and control parameters are made available to the laboratory operator through a custom software interface based on the dSpace Control Desk tool, running on a remote computer.

5. Experimental results and discussions

The laboratory test bench, described in the previous Section, has been used to analyse the real effectiveness of the EMSs for the vehicle power-train, running on standard driving cycles in real operative conditions. On this regard, the experimental tests of the EMSs, previously introduced, can take advantage of the parameters of Table 4, which have been optimized through the simulation procedure reported in Section 3.

A first experimental test has been carried out, for the *Ke Strategy*, with the propulsion system running on a plain road ECE-15 driving cycle. The main experimental results for this test are reported in the following Fig. 13.

In particular, the considered EMS involves that the higher is the values of vehicle speed (A), the lower is the EDLCs Voltage and SoC (B). In fact, due to the PI controller of V_{SC}, reported in the block scheme of Fig. 5, the EDLCs voltage and SoC reach their lowest values of 50 V and 65%, in the last part of the driving cycle, just before the longest regenerative phase occurs (B). For the same reasons, high values of EDLCs Voltage and SoC are related to the resting phases of the driving cycle at zero speed. In this case, the maximum values of 120 V and 80% (B) are obtained, just before the last and longest acceleration phase occurs (A). Fig. 13 (C) shows the behaviour of battery pack, in terms of Voltage and SOC, as a consequence of the above EDLCs operations. A maximum total current on the DC-Link side, I_{DC}, of about 50 A (D) is evaluated for this driving cycle. This value corresponds to a maximum battery discharging current, I_{Batt}, of 35 A (E). This means that the use of EDLCs involves a reduction of maximum battery discharging current of about 30% (D). Moreover, during the steady state operations, the EDLCs current reported on the DC-Link side, I'_{SC}, results rather low (E). In fact, during those operations, the mechanical power is mainly supplied by the electric power coming from the battery pack. In fact, the first term of battery current reference, $I^{*'}_{Batt}$, which is reported in the functional scheme of Fig. 5, is evaluated on the base of the mechanical power associated to road and aerodynamic resistant forces. Finally, during the regenerative operations, the great part of electric power is directed towards the EDLCs, with a reduction of the effects of high regenerative

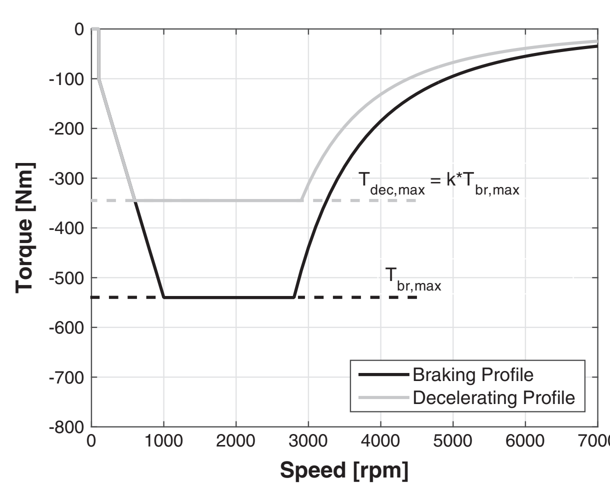

Fig. 12. Electric Drive braking and decelerating profiles.

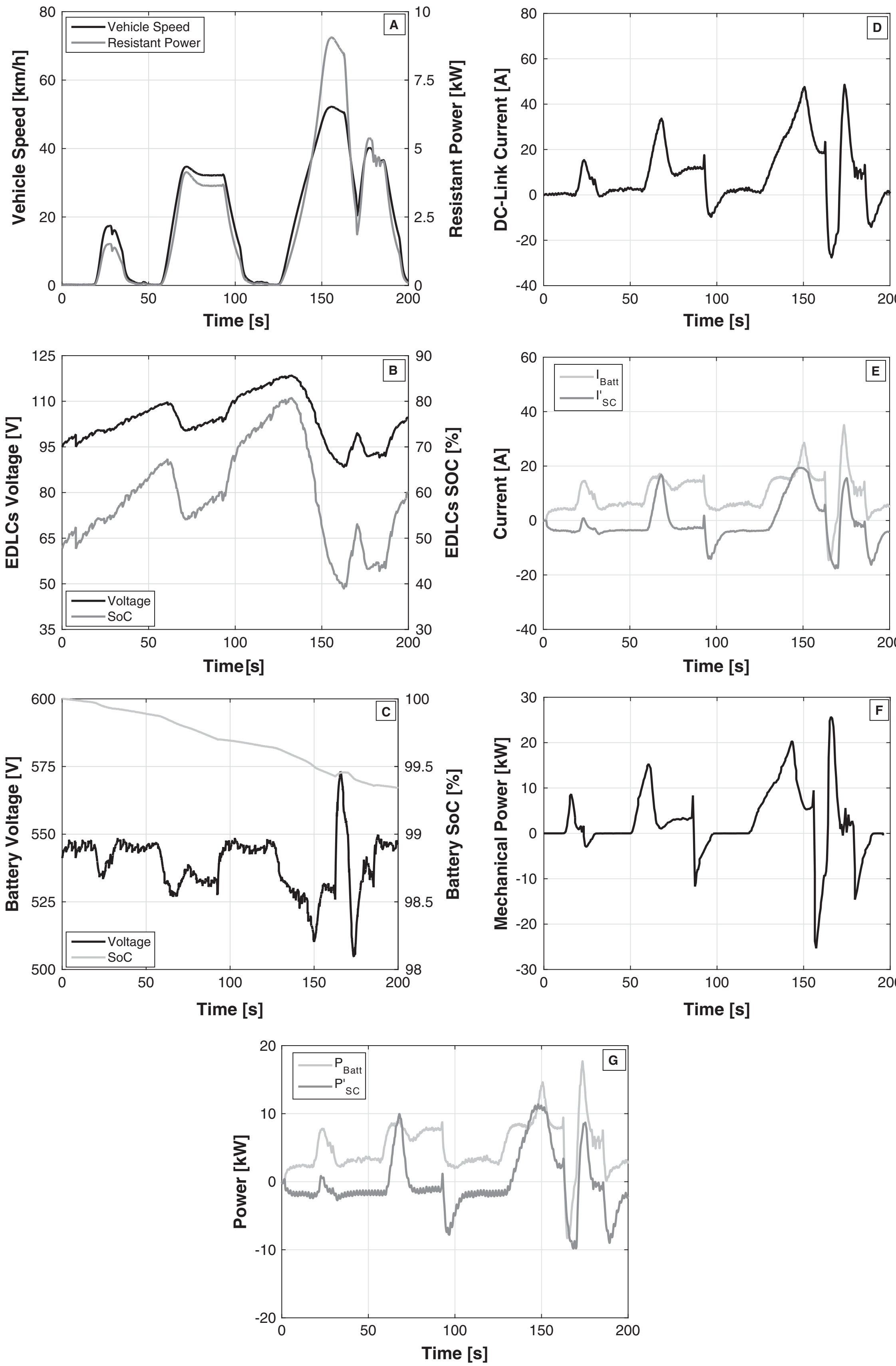

Fig. 13. Experimental results: Vehicle Speed and Road Resistant Power (A), EDLCs Voltage and SoC (B), Battery Pack Voltage and SoC (C), DC-Link Current (D), Battery and EDLCs current on the DC-Link side (E), Mechanical Power (F), Battery and EDLCs power on the DC-Link side (G) vs. time for the ECE-15 driving cycle, on plain road, with Ke Strategy.

Table 6
Experimental results of EMSs effectiveness on the considered driving cycles.

Effectiveness	ECE-15	ECE-15 5%	NEDC
Th Strategy	44%	12%	10%
EWMA Strategy	50%	34%	8%
Ke Strategy	53%	23%	13%

currents on battery durability (E). Therefore, battery negative power values (F, G) are observed only during the decelerating phase at the maximum speed of the driving cycle, when the DC link total regenerative current reaches the value of about −30 A (D). In this case, the contribution of the EDLCs is limited by the Maximum EDLCs Discharging Current Limit, which has been preliminary set at −100 A, on the EDLCs side of the power converter.

The same experimental test has been also performed without the use of the EDLCs module to evaluate, on the base of the Eq. (3), the experimental effectiveness of the considered EMS. In particular, after five consecutive repetitions of each ECE-15 driving cycle, the obtained value of experimental effectiveness is 53%. As a matter of fact, this value can be considered equivalent to the effectiveness value of 57%, which has been calculated through the simulation model, for the practical application of this work.

Similar tests have been carried out through the laboratory test bench, by using the other EMSs, considered in this paper, on the driving cycles described in Section 3. Also in these cases, the EMSs are based on the parameters of Table 4 that have been preliminary identified, in simulation environment, through the optimization procedure. The main results, in terms of experimental effectiveness for the considered driving cycles, are summarized in Table 6.

The experimental results, reported in the above Table, show that for the ECE-15 driving cycle, on plain road, the lowest value of effectiveness is obtained with the *Th EMS*. In fact, in this case, the maximum battery current is limited by a saturation block based on a constant current threshold I_{Th} of 10 A. In addition, the regenerative operations are managed by using the EDLCs without any control on their state of charge. In this case, a resulting effectiveness value of 44% is obtained. For this driving cycle, the best effectiveness value is evaluated with the *Ke Strategy*. In fact, as shown by the results reported in Fig. 13, this EMS allows the optimization of the EDLCs state of charge as a function of the vehicle speed, through the use of the EDLCs voltage PI control. For this reason, during regenerative and acceleration phases, the great part of electric power is respectively received or supplied by EDLCs. The experimental results for the ECE-15 driving cycle, with positive road slope of 5%, have shown a slight decrease of effectiveness with all the EMSs analysed, in comparison with the case of plane road. This is mainly due to the fact that, in this case, higher values of electric power are required by the driving cycle and, as a consequence, the related effect of the EDLCs charging/discharging power on the evaluated effectiveness is reduced. For this test, the lowest effectiveness value of 12% is still obtained with the *Th Strategy*, whereas the highest effectiveness of 34% is evaluated for the *EWMA Strategy*. Also in this case, the maximum experimental effectiveness is similar to the effectiveness value of 37%, obtained through the simulation model, described in Section 3. For this driving cycle, the low values of regenerative electric power limit the effectiveness of the *Ke Strategy,* because of the reduced effect of using the V_{SC} PI Control during the decelerating phases. The last experimental test is related to the effectiveness evaluation of the EMSs analysed in this paper for the NEDC driving cycle. In this case, a general decrease of effectiveness, compared to the other two considered driving cycles, is observed for both simulation and experimental results. In fact, as already mentioned in the discussion related to the simulation results of Fig. 7, the low effectiveness values are justified by the high electric power requirement of the NEDC driving cycle during its extra-urban phase. However, the highest value of effectiveness of 13% is obtained with the *Ke Strategy*, which ensures the highest contribution of EDLCs electric power, during the transient acceleration phases, and optimizes the regenerative operations related to the extra-urban phase by means of the V_{SC} PI Control as a function of the speed. Also for the NEDC driving cycle the maximum experimental effectiveness is similar to the effectiveness value of 16% obtained through the simulation model, described in Section 3. In this case, the lowest effectiveness of 8% is obtained with the *EWMA Strategy*, which is affected by the high variation in the speed profile of extra-urban part of the driving cycle.

The comparison derived from the simulation and experimental results suggests that the performance of the described energy management strategies depends on the considered driving cycles. In particular, the *Th strategy* has shown acceptable performance, in terms of effectiveness, only for driving cycles characterized by low power demand. The *EWMA* strategy has generally shown good performance, but its effectiveness falls down when high variations of power are required by the driving cycles. The *Ke strategy* has evidenced good performance in the analysed driving cycles, with a slight decrease of effectiveness for driving cycles with high average power demand. For the above reasons, the choice of the proper EMS should be carry out on the base of the expected vehicle mission.

The experimental results, reported in this section, are consistent with the state of art described in the Introduction Section, even though the scientific literature evaluates the advantages of proper energy management strategies in terms of battery durability through expected results obtained with simulation procedures [20–22].

These results show that combining battery packs with modules of super-capacitors involves various positive aspects. In particular, those hybrid storage systems can benefit, on one hand, from the possibility to deal with high power peaks, and, on the other hand, from the ability, given by high specific power units such as EDLCs, to reduce the effects of high charging/discharging current values on battery durability. This fundamental aspect needs to be carefully taken into account to guarantee the longest lifespan of the onboard energy storage system, represented by the battery pack.

6. Conclusions

The performance of a hybrid energy storage system, composed of ZEBRA batteries and electric double layer capacitors (EDLCs), has been evaluated in this paper, through a 1:1 scale laboratory test bench, to simulate real road urban commercial vehicle operations.

The integration between the two storage units has been realized by means of a bidirectional DC/DC power conversion system, able to balance the electric power between batteries and super-capacitors.

The operations of the hybrid energy storage system, when supplying the considered vehicle on urban driving cycles, has been controlled through three main rule based energy management strategies. The performance of each EMS have been evaluated and compared through the well known effectiveness objective function, which takes into account the effects of charging/discharging current peaks on the battery pack durability.

Before running experimental tests, a quasi-static simulation model of the full power train, comprehensive of vehicle inertia, has been deployed in Matlab-Simulink environment. This model has made possible the off-line tuning and optimization of EMS parameters, useful to obtain the maximum performance of the hybrid energy storage system in terms of effectiveness.

Experimental results have been carried out in terms of the main electric, mechanical and thermal parameters for both ECE-15 and NEDC driving cycle. In particular, for the ECE-15 driving cycle on plain road, the effectiveness values have been assessed in the range 44–53%. In this case, the best result has been obtained with an optimal use of the EDLCs during regenerative and acceleration phases due to the *Ke Strategy*. In a similar way, on the NEDC driving cycle, which takes into account the extra-urban phase, the maximum effectiveness value of 13% has been evaluated with the *Ke Strategy*. With a road slope of 5%, on the ECE-15 driving cycle, the same strategy has shown lower effectiveness value, because of the low power regenerative operations; whereas the best effectiveness value of 34% has been obtained with the *EWMA Strategy*.

Finally, the numerical modeling and laboratory experimental results of this paper have shown the importance to verify the energy management strategies of hybrid storage systems on laboratory test benches, before working on road vehicle prototypes. In fact, this procedure results in a reduction of experimentation time and general costs. Vehicle manufacturers can also take advantage of the results reported in this paper, by considering similar hybrid storage systems to power other types of vehicles, but also following the same methodology to evaluate the performance of other architecture.

Acknowledgements

The authors gratefully acknowledge Mr. Antonio Rossi and Mr. Salvatore Gabriele, technicians of Istituto Motori, for their cooperation in realization of the experimental apparatus and running of laboratory tests. The authors also acknowledge Mr. Silvio Lamberti for his cooperation in laboratory and simulation tasks during his master degree thesis at Istituto Motori.

References

[1] Zhang K, Batterman S. Air pollution and health risks due to vehicle traffic. Sci Total Environ 2013;451:307–16.
[2] Lawrence BD. Sustainable mobility: a vision of our transport future. Nature 2013;497(7448):181–2.
[3] Jacobson MZ. Review of solutions to global warming, air pollution, and energy security. Energy Environ Sci 2009;2(2):148–73.
[4] Scrosati B, Garche J, Tillmetz W. Advances in battery technologies for electric vehicles. Woodhead Publishing; 2015.
[5] Faggioli E, et al. Supercapacitors for the energy management of electric vehicles. J Power Sources 2009;84(2):261–9.
[6] Pay S, Baghzouz Y. Effectiveness of battery-supercapacitor combination in electric vehicles. In: IEEE power tech conference proceedings; 2003.
[7] Zhang C, et al. Charging optimization in lithium-ion batteries based on temperature rise and charge time. Appl Energy 2017;194:569–77.
[8] Khaligh A, Li Z. Battery, ultracapacitor, fuel cell, and hybrid energy storage systems for electric, hybrid electric, fuel cell, and plug-in hybrid electric vehicles: state of the art. IEEE Trans Veh Technol 2010;59(6):2806–14.
[9] Blanes JM, et al. Electric vehicle battery life extension using ultracapacitors and an FPGA controlled interleaved buck–boost converter. IEEE Trans Power Electr 2013;28(12):5940–8.
[10] Shen J, Dusmez S, Khaligh A. Optimization of sizing and battery cycle life in battery/ultracapacitor hybrid energy storage systems for electric vehicle applications. IEEE Trans Ind Inform 2014;10(4):2112–21.
[11] Zhang F, et al. A high-performance supercapacitor-battery hybrid energy storage device based on graphene-enhanced electrode materials with ultrahigh energy density. Energy Environ Sci 2013;6(5):1623–32.
[12] Deepak DP, et al. Hybrid energy storage: the merging of battery and supercapacitor chemistries. Chem Soc Rev 2015;44(7):1777–90.
[13] Arbizzani C, et al. Lithium-ion batteries and supercapacitors for use in hybrid electric vehicles - lithium batteries: advanced technologies and applications; 2013. p. 265–75.
[14] Shah VA, et al. Review of ultracapacitor technology and its applications. In: Proceedings of the 15th national power system conference; 2008.
[15] Pawan S, Bhatti TS. A review on electrochemical double-layer capacitors. Energ Convers Manage 2010;51(12):2901–12.
[16] Lukic SM, et al. Energy storage systems for automotive applications. IEEE Trans Ind Electron 2008;55(6):2258–67.
[17] Cao J, Emadi A. A new battery/ultracapacitor hybrid energy storage system for electric, hybrid, and plug-in hybrid electric vehicles. IEEE Trans Power Electr 2012;27(1):122–32.
[18] Kohler TP, Buecherl D, Herzog HG. Investigation of control strategies for hybrid energy storage systems in hybrid electric vehicles. In: IEEE vehicle power and propulsion conference; 2009. p. 1687–93.
[19] Noshin O, et al. Electrical double-layer capacitors in hybrid topologies—assessment and evaluation of their performance. Energies 2012;5(11):4533–68.
[20] Guidi G, Undeland TM, Hori Y. Effectiveness of supercapacitors as power-assist in pure ev using a sodium-nickel chloride battery as main energy storage. In: Proceedings of the 24th international battery, hybrid and fuel cell electric vehicle symposium (EVS-24); 2009.
[21] Ziyou S, et al. Multi-objective optimization of a semi-active battery/supercapacitor energy storage system for electric vehicles. Appl Energy 2014;135:212–24.
[22] Zhang S, Xiong R, Cao J. Battery durability and longevity based power management for plug-in hybrid electric vehicle with hybrid energy storage system. Appl Energy 2016;179:316–28.
[23] Carter R, Cruden A, Hall PJ. Optimizing for efficiency or battery life in a battery/supercapacitor electric vehicle. IEEE Trans Veh Technol 2012;61(4):1526–33.
[24] Veneri O, Capasso C, Patalano S. Experimental study on the performance of a ZEBRA battery based propulsion system for urban commercial vehicles. Appl Energy 2017;185(2):2005–18.
[25] Capasso C, et al. Experimentation with a ZEBRA plus EDLC based hybrid storage system for urban means of transport. In: IEEE international conference on electrical systems for aircraft, railway, ship propulsion and road vehicles (ESARS); 2015.
[26] Vulturescu B, Trigui R, Lallemand R, Coquery G. Implementation and test of a hybrid storage system on an electric urban bus. Transp Res Part C: Emerg Technol 2013;30:55–66.
[27] Castaings A, et al. Comparison of energy management strategies of a battery/supercapacitors system for electric vehicle under real-time constraints. Appl Energy 2016;163:190–200.
[28] Spyker RL, Nelms RM. Classical equivalent circuit parameters for a double-layer capacitor. IEEE Trans Aero Electr Sys 2000;36(3):829–36.
[29] Luo FL, Hong Y. Advanced dc/dc Converters. CRC Press; 2003.
[30] Rashid M. Power electronics handbook: devices, circuits and applications. Academic Press; 2010.